British Journal of Pharmacology (1996) 119, 647-654

Extracellular site for econazole-mediated block of Ca^{2+} release-activated Ca^{2+} current (I_{crac}) in T lymphocytes

[1]Edward P. Christian, Katherine T. Spence, James A. Togo, Pauline G. Dargis & *Edward Warawa

Departments of Pharmacology and *Medicinal Chemistry, Zeneca Pharmaceuticals, Wilmington, Delaware 19850-5437, U.S.A.

1 Standard whole cell patch clamp recording techniques were used to study the pharmacological characteristics and site of econazole-mediated inhibition of calcium release-activated calcium current (I_{crac}) in the human leukaemic T cell line, Jurkat.

2 Extracellularly applied econazole blocked I_{crac} in a concentration-dependent manner ($IC_{50} \approx 14$ μM). Block developed over a relatively slow timecourse of 30-60 s (10 μM), and only partially reversed over minutes.

3 Econazole dialysed from the pipette into the cytosol at concentrations ranging from 0.1 to 30 μM did not reduce I_{crac}, or quantitatively affect I_{crac} block by extracellularly applied econazole.

4 A less lipophilic quaternary iodide derivative of econazole was synthesized to retard absorption through the cell membrane. When applied extracellularly, this compound blocked I_{crac} in a concentration-dependent manner with onset kinetics comparable to econazole.

5 Results with intracellularly dialysed econazole and the quaternary econazole derivative provide convergent evidence that econazole blocks I_{crac} via an extracellular interaction.

6 The inability of intracellularly applied econazole to inhibit I_{crac} argues against the notion that econazole inhibits capacitative Ca^{2+} entry pathways secondary to its known inhibitory effects on cytochrome P-450.

Keywords: Calcium current; depletion-activated calcium current; calcium release-activated calcium current; econazole; T lymphocyte; Jurkat cell; cytochrome P-450

Introduction

A major pathway for sustaining Ca^{2+} signals and refilling microsomal stores in a variety of non-excitable cells has been termed capacitative Ca^{2+} entry (Putney, 1990), based on its apparent regulation by the Ca^{2+} levels within these stores. Whole cell patch clamp studies first identified a highly selective Ca^{2+} entry pathway in T lymphocytes and provided evidence that it was the pathway for capacitative Ca^{2+} influx (Lewis & Cahalan, 1989). Subsequently, more detailed whole cell studies have revealed very similar biophysical profiles for selective Ca^{2+} currents activated by Ca^{2+} store depletion in both mast cells (Hoth & Penner, 1992; 1993) and in T cells (McDonald *et al.*, 1993; Zweifach & Lewis, 1993; 1995; Premack *et al.*, 1994). Both are now commonly referred to by the acronym that was originally assigned to the mast cell current (i.e., I_{crac}; Hoth & Penner, 1992).

Despite growing research interest in the biophysics, regulation, and physiological roles of capacitative Ca^{2+} entry, knowledge regarding the pharmacology of these pathways is rudimentary, and the molecular blocking mechanisms underlying activity of the small number of known inhibitors remain unsettled. The most widely acknowledged organic blockers of capacitative Ca^{2+} influx pathways are a class of N_1-substituted imidazole antimycotics, such as econazole and miconazole (Alvarez *et al.*, 1991; 1992; Mason *et al.*, 1993; Vostal & Fratantoni, 1993; Koch *et al.*, 1994), and the closely related compound, SK&F 96365 (Merritt *et al.*, 1990; Mason *et al.*, 1993). A concentration-dependent blocking action of certain imidazole compounds has also been confirmed at the level of I_{crac} with patch clamp techniques in T cells and mast cells (Chung *et al.*, 1994; Franzius *et al.*, 1994).

Econazole and other imidazole antimycotics were originally recognized as inhibitors of cytochrome P-450 in the micromolar range (Rodrigues *et al.*, 1987; Ballard *et al.*, 1988; Murray & Zaluzny, 1988). The observation that these compounds also inhibit capacitative Ca^{2+} influx prompted a hypothesis causally associating this to the cytochrome P-450 inhibition (Alonso *et al.*, 1991; Alvarez *et al.*, 1991; 1992; Montero *et al.*, 1991; Sargeant *et al.*, 1992). Thus cytochrome P-450 was also implicated in the molecular signalling pathway linking store depletion to the induction of capacitative Ca^{2+} entry. Several subsequent studies have provided contrasting evidence, arguing against the involvement of cytochrome P-450 in imidazole-mediated inhibition of capacitative Ca^{2+} influx (Vostal & Fratantoni, 1993; Koch *et al.*, 1994). However, these studies failed to clarify other possible blocking mechanisms or sites of action for the imidazole-mediated inhibition of capacitative Ca^{2+} entry.

In the present study we sought to discriminate whether econazole blocks I_{crac} in Jurkat T cells from an extracellular or intracellular site. We applied econazole intracellularly through patch pipettes and compared the effects to those of extracellularly applied econazole. To complement this, we evaluated the effects on I_{crac} of an extracellularly applied quaternary salt derivative of econazole with substantially reduced ability to partition into the lipid membrane. Results have provided convergent evidence that econazole blocks I_{crac} by an extracellular interaction, and thus argue strongly against the prior hypothesis invoking cytochrome P-450 in this process. Some of the results described here have been published previously in abstract form (Christian *et al.*, 1995).

Methods

Cell culture

Studies were performed in the established cell line of human leukaemic E6-1 Jurkat T cells (ATCC T1B 152). Cell cultures were maintained at log phase growth between 0.1 and 1.5×10^6 cells ml^{-1} in medium containing RPMI 1640 (Mediatech, Herndon, VA) and 10% foetal bovine serum (HyClone, Logan, UT). Cell cultures were incubated at 37°C in an atmos-

[1] Author for correspondence.

phere containing 5% CO_2. For recording, cells in a 150 μl aliquot of media were allowed to adhere to a poly-D-lysine-coated plastic culture dish for 3–5 min before being switched to experimental solutions.

Electrophysiology

Experiments were performed at room temperature (22–24°C) in a static bath chamber mounted on the stage of a Nikon Diaphot inverted microscope. The standard whole cell configuration of the patch clamp technique was used for recordings (Hamill *et al.*, 1981). Pipettes were fabricated from thin wall borosiclicate glass (1.5 mm o.d., 1.12 mm i.d.; World Precision Instruments, Sarasota, FL) on a Flaming-Brown P-87 Puller (Sutter Instruments, Novato, CA), Sylgarded (Dow Corning, Midland, MI) near the tip, and polished to a d.c. resistance of 2–8 MΩ. Membrane currents were amplified with either an Axopatch 1B or 200A amplifier (Axon Instruments, Foster City, CA), low-pass filtered at 1 kHz with an 8-pole Bessel filter, and then digitized at 3–5 kHz as computer files with a TL-1 interface (Scientific Solutions, Solon, OH). A full unfiltered record of currents recorded in the experiment was also pulse encoded to VCR tape, so that extended data epochs could be digitized off-line for some analyses. Voltage clamp protocols were implemented and data acquisition performed with pClamp 6.0 software (Axon Instruments).

The pipette current was zeroed before a seal was formed. The resistance of patch seals was >10 GΩ. Whole cell capacitance was nulled with circuitry in the amplifier. Following initial attainment of the whole cell configuration, and at subsequent intervals during the experiment, uncompensated capacitive current transients to −1 mV, 10 ms steps were obtained to determine whole cell capacitance (C_m = integral of capacitive transient), and series resistance [R_s = decay τ of capacitive transient (C_m^{-1})]. Cells were rejected if either of these parameters varied by >10% during the experiment. Series resistance compensation was not used in most experiments: current was generally <100 pA, C_m <40 pF and R_s was <15 MΩ producing worst case predicted voltage errors of <1.5 mV, and low pass filtering effects with a first order rolloff frequency >265 Hz. Likewise, command potentials were not corrected for the ≈−10 mV junction potential calculated (Barry & Lynch, 1991) between the standard pipette and bath solutions. None of these measurement errors were judged to have significant impact on the conclusions reached in this study.

Voltage clamp protocols used a holding potential of 0 mV to minimize the electrochemical gradient for Ca^{2+} influx. To monitor I_{crac}, repetitive 200 ms voltage steps to −100 mV or 200 ms ramps between −150 and +20 mV were delivered at frequencies varying from 0.1 to 1 Hz. Under these conditions, stable recordings of I_{crac} were attainable for usually >10 min. Raw currents shown in figures were not leak subtracted.

Solutions and drugs

Recording solutions were (in mM); extracellular: NaCl 160, KCl 4.5, $CaCl_2$ 2, $MgCl_2$ 1, D-glucose 5, HEPES 5, pH to 7.4 with NaOH; pipette: Cs-aspartate 140, $MgCl_2$ 2, EGTA 10, HEPES 10, pH to 7.2 with CsOH. The pipette solution was hyposmotic (≈305 mOsm), relative to the extracellular solution (≈320 mOsm). All salts for solutions were purchased from Sigma (St. Louis, MO). In the 'Ca^{2+}-free' or '0 mM Ca^{2+}' extracellular solution, Ca^{2+} was substituted with equimolar Mg^{2+}. Solutions were sterile filtered (pore size: 0.22 μm) and stored as aliquots (4°C for extracellular; −20°C for intracellular) for up to one month before use.

Econazole (nitrate salt; Sigma) was dissolved (5 mM) in dimethylsulphoxide (DMSO) and stored as frozen stock aliquots for final dissolution in extracellular buffer on the day of experiments. Previous control experiments in our laboratory (unpublished) have verified that the highest final concentration of DMSO used has no effect on I_{crac} amplitude or stability.

A quaternary salt of econazole (econazole methiodide; 1-[2,4-dichloro-β-(4-chlorobenzyloxy)]phenethyl imidazole methiodide) was synthesized in-house with the objective of retarding partitioning into the membrane and thereby decreasing drug access to a putative intracellular receptor site. The octanol:water partitioning ratio (P) at pH 7.4 was determined to be 1.0 for econazole methiodide (log P=0), and 346 for econazole (log P=2.54). Econazole methiodide was solubilized and applied in an identical manner to econazole. Details of the synthesis of econazole methiodide were as follows: a solution of econazole, 0.83 g (2.17 mmol), in 20 ml dry acetone was treated with iodomethane, 3.08 g (21.7 mmol). This solution was stirred in a stoppered flask overnight at ambient temperature. Thin layer chromatographic (t.l.c.) analysis on silica gel plates, eluting with 10% methanol-methylene chloride, indicated the complete absence of econazole and exhibited a single component at R_F=0.5. The solvent was removed *in vacuo* by a rotary evaporator to furnish a solid which was triturated with ether and collected by filtration. After drying overnight in a drying pistol at 10 mtorr (ambient temperature), the yield was 1.05 g (93%): m.p. 158–160°C. As evidenced by nuclear magnetic resonance (n.m.r.), quaternization with iodomethane gave a monomethiodide salt which existed as regio isomers, alkylation having occurred at either N-1 or N-3 of the imidazole [^{1}Hn.m.r. (300 MHz, $CDCl_3$) analysis: δ 3.87 (s, CH_3), 3.34 (s, CH_3), a mixture (2:1) of regio salts; calculated values for $C_{18}H_{15}C_{13}N_2O{\cdot}CH_3I$: C, 43.58; H, 3.46; N, 5.35; measured values: C, 43.52, 43.57; H, 3.53, 3.53; N, 5.23, 5.21].

Extracellular solutions were switched with a linear array of gravity fed glass-lined tubes (100 μm i.d.; Hewlett Packard Corp., Wilmington, DE) controlled by a system of solenoid valves (BME Systems, Baltimore, MD). The tube containing the desired solution was localized <1 cell diameter from a cell before the solenoid was activated. This system enabled complete exchange of extracellular solutions in <200 ms, based on the timecourse for removal of Ca^{2+}-selective flux through I_{crac} channels (Christian *et al.*, 1996).

Data analysis

I_{crac} amplitude was measured by use of p-Clamp software. Three to five current epochs were digitally averaged for all measurements. In the case of −100 mV voltage steps, the measurement commenced 10 to 15 ms after step onset to remove any contribution of uncompensated capacitive transients. From this point current was measured over a 2–3 ms digitally averaged interval. In the case of voltage ramps, current was measured from a digitally averaged interval between −101 and −99 mV on the voltage ramp.

For analysis I_{crac} was quantified as the calcium-selective component of current as follows:

$$I_{crac} = I_{(2\ mM\ Ca^{2+}out)} - I_{(0\ mM\ Ca^{2+}out)}$$

This was based on the rationale that the magnitude of current in nominally Ca^{2+}-free (0 mM $Ca^{2+}{}_{out}$)-containing extracellular solution was generally within 10% of the current measured immediately after accessing the whole cell mode in 2 mM extracellular Ca^{2+}, before I_{crac} induction (e.g., Figures 3 and 5). The current in 0 mM Ca^{2+}, hereafter referred to as 'leak' current, was sampled near the beginning of each experiment and then at least once more before the end of a recording. Data were rejected if leak current varied by >10% during the experiment.

Origin software (Version 3.73; Microcal Inc., Northhampton, MA) was used to construct figures and to iteratively fit data to monoexponential decay functions, by use of a Marquardt-Levenberg non-linear least-squares algorithm. Greater than 99% of the total variance was accounted for by all fits. All values are expressed as the mean ± s.e.mean unless otherwise stated. Analysis of variance (ANOVA) was used to test differences between multiple means. P<0.05 was defined as a significant effect for all statistical tests.

Results

Characteristics of I_{crac} *and its block by extracellularly applied econazole*

The E6-1 Jurkat cell line was used, since I_{crac} has been well characterized in these cells at the biophysical level (McDonald *et al.*, 1993; Zweifach & Lewis, 1993; 1995; Premack *et al.*, 1994), and it has previously been shown to be blocked by an imidazole structurally similar to econazole (i.e., SK&F 96365; Chung *et al.*, 1994). Following attainment of the whole cell configuration with control extracellular and pipette solutions, repeated (0.1 to 1 Hz) 200 ms steps to −100 mV, or ramps between −150 mV and +20 mV typically revealed a peak inward current that increased over 2–5 min to an asymptotic level. This increase in current was taken to represent the induction of I_{crac} following microsomal Ca^{2+} store depletion. The latency of this process presumably reflected the time required for intracellular dialysis of the high Ca^{2+} buffered pipette solution, passive Ca^{2+} store depletion, and the subsequent yet unresolved intracellular signalling events leading to I_{crac} activation (Zweifach & Lewis, 1993; Premack *et al.*, 1994).

I_{crac} recorded under our conditions (see also Christian *et al.*, 1996) exhibited properties analogous to those documented previously for I_{crac} in Jurkat cells (McDonald *et al.*, 1993; Zweifach & Lewis, 1993; 1995; Premack *et al.*, 1994), including: low current density (1.51 ± 0.16 pA pF^{-1} at −100 mV and 2 mM external Ca^{2+}; $n = 21$), dependence on extracellular Ca^{2+} (Figures 1, 3 and 5), greater Ca^{2+} than Ba^{2+} permeation, time- and voltage-independent activation during voltage steps, inability to reverse at depolarized potentials (Figure 1b), inward rectification of the I/V relationship at hyperpolarized potentials, rapid (<200 ms) block by millimolar concentrations of divalent metals such as Ni^{2+} and Cd^{2+}, and rapid inactivation during 200 ms, hyperpolarizing voltage steps.

The effects on I_{crac} of a range of extracellularly applied econazole concentrations (0.1–30 μM) were studied (Figure 1). Concentrations >30 μM were not evaluated due to solubility limitations. Econazole produced a concentration-dependent reduction in I_{crac}, as measured by voltage steps or ramps (e.g., Figure 1a and b). Block onset kinetics were relatively slow (see below), so ≥1 min of equilibration time was allowed for each concentration before the current was measured. The steady state I_{crac} amplitude measured during either ramps or steps was normalized to control amplitude as a % inhibition value for each econazole concentration. The mean normalized current measurements from 21 cells were fitted to a logistic function, yielding an IC_{50} of 13.5 μM, and a slope factor of 1.07 (Figure 1c). The highest econazole concentration tested (30 μM) caused a 71 ± 11 ($n = 13$) % inhibition of the peak I_{crac}.

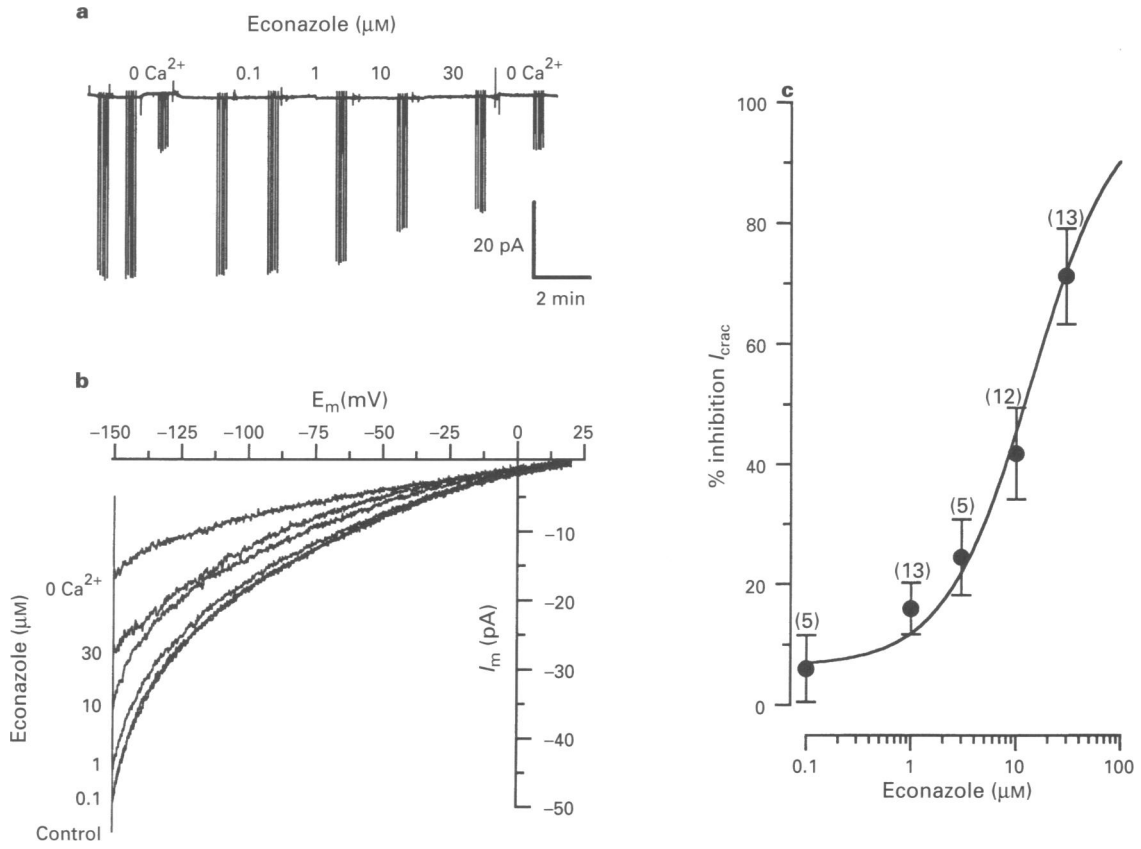

Figure 1 Concentration-dependent block of I_{crac} by econazole in Jurkat cells. (a) Continuous record of whole cell current recorded during removal of extracellular Ca^{2+} ($0\,Ca^{2+}$) or during application of increasing extracellular concentrations of econazole. The record was filtered at 50 Hz and digitized at 100 Hz. Downward deflections are current responses to −150 to +20 mV, 200 ms voltage ramps (holding potential: 0 mV). Ramps were delivered in groups of five at 0.2 Hz, commencing >1.5 min after each solution exchange to allow for equilibration of drug effect (see Figure 2). (b) Expanded superimposed traces of current responses to ramps from experiment in (a) plotted as a function of command voltage. Records were filtered at 1 kHz and digitized at 5 kHz. Treatments are indicated to the left of corresponding trace. Each trace is a digital average of the five individual currents obtained from each group shown in (a). Currents are not leak subtracted. (c) Mean concentration-response relationship for I_{crac} inhibition by econazole. Each data point represents the mean ± s.e.mean (n in parentheses) normalized % of I_{crac} inhibition at the indicated extracellular econazole concentration. I_{crac} was measured at −100 mV from averaged voltage ramps using the protocol shown in (a and b), or from the peak current (10 ms after step onset) obtained during voltage steps (average of five −100 mV, 200 ms steps; holding potential: 0 mV). See Methods for further details of I_{crac} measurement and normalization procedures. The solid line is a fit to the logistic function: $100/[1 + (IC_{50}/x)^n]$, where x is econazole concentration, IC_{50} is the concentration producing 50% I_{crac} block, and n is the slope factor of the line. Parameters of fit were: $IC_{50} = 13.5\,\mu M$; $n = 1.07$.

The temporal development of steady-state block by econazole occurred slowly, with the attainment of steady-state block during application of 10 μM econazole requiring up to one min (Figure 2). Moreover, upon econazole washout, the block reversed on a protracted time scale (>3 min) that made full recovery difficult to monitor (e.g., Figure 5). This kinetic behaviour contrasted notably with the rapid onset and reversal (<200 ms) of I_{crac} block we have previously obtained with this same drug delivery system for inorganic cations such as Ni^{2+} and Cd^{2+} (Christian *et al.*, 1996).

The kinetics for block onset during exposure to 10 μM econazole were quantified from the peak current measured during repetitive −100 mV, 200 ms steps delivered at 0.5 Hz. Following application of 10 μM econazole, I_{crac} decreased with a timecourse that was well fitted by monoexponential kinetics ($\tau = 13.0 \pm 1.4$ s; $n = 6$). To ascertain mean ± s.e.mean values for I_{crac} decay time-locked to econazole application, each sequential current measurement was normalized as a fraction of the maximal steady-state blocked I_{crac} amplitude, and these values were averaged over the six experiments for each successive 0.5 s time point after drug delivery had commenced (Figure 2b). This graphical format demonstrates that the kinetics for onset of econazole block varied little between the experiments.

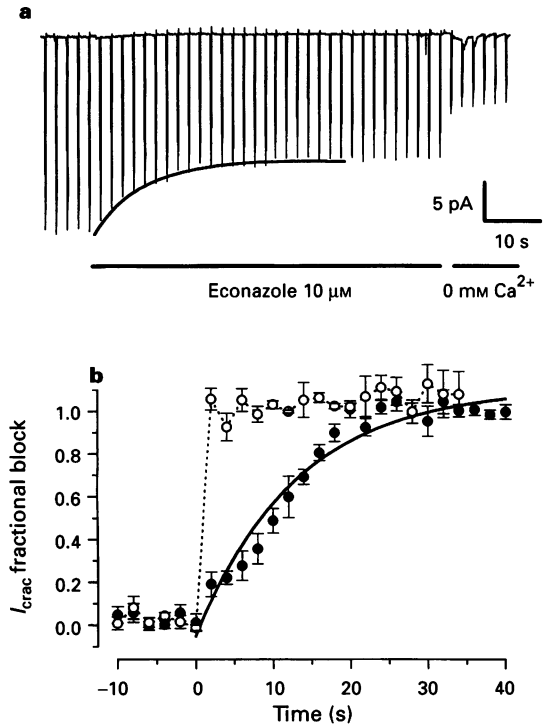

Figure 2 Kinetics for the onset of I_{crac} block by econazole. (a) Continuous current trace obtained from a voltage clamp recording during the initial application of econazole (10 μM; bar), and subsequent removal of extracellular Ca^{2+}. Downward deflections are current responses to −100 mV, 100 ms steps delivered at 0.5 Hz (holding potential: 0 mV). Solid line is a single exponential fit ($\tau = 12.2$ s) to the econazole-mediated block of the peak currents during the steps. In contrast, Ca^{2+} removal (replacement by equimolar Mg^{2+}) caused a rapid reduction of current to its steady state minimum within the first 2 s interval between steps. (b) Summary data obtained from protocol in (a) showing the timecourse of mean ± s.e.mean I_{crac} reduction resulting from extracellular application of 10 μM econazole (●; $n = 6$) or Ca^{2+} removal (○; $n = 3$) at time 0. In each experiment, peak I_{crac} amplitude was measured during −100 mV steps at sequential 2 s time points, and normalized as a fractional block value between control amplitude (=0) and steady-state minimum amplitude in econazole or 0 Ca^{2+} (=1). Graph shows the average (± s.e.mean) of the fractional values fixed to the time of solution exchange (0 time). The solid line is a monoexponential fit to the mean econazole datapoints ($\tau = 13.1$ s). Note that mean I_{crac} decayed to an asymptotic minimum within 2 s of Ca^{2+} removal, analogous to the example in (a).

Data included in Figure 2 additionally provide proof that the relatively slow timecourse for onset of econazole block could not be attributed to the mechanics of the drug delivery system itself: switching from extracellular 2 mM to 0 mM Ca^{2+} with this system reduced current to an asymptotic leak current level within the first two-second sampling interval of the exchange.

Effects of intracellularly applied econazole on I_{crac}

The relatively slow kinetics for the development of and recovery from econazole-induced I_{crac} block in combination with the hydrophobicity, and other known biochemical actions of econazole (e.g., cytochrome P-450 inhibition; see Discussion) together raised the possibility that block was exerted indirectly from an intracellular site. To distinguish between an intracellularly vs. extracellularly mediated action, econazole (0.1–30 μM) was dialysed intracellularly via the recording pipette. We postulated that intracellular block by econazole would be manifested either by a failure of I_{crac} to develop to normal amplitude, or alternatively by a progressive decay of I_{crac} as the compound diffused into the cell.

Six experiments were conducted in which I_{crac} was monitored during extended periods, ranging from 18.2 to 33.8 min after the whole cell configuration had been obtained with recording pipettes containing 30 μM econazole (Figure 3). Figure 3a shows a representative experiment in which I_{crac} developed within 4 min to an asymptotic amplitude that remained stable for the duration of the experiment (≈29 min post break-in). The steady-state I_{crac} density of 1.20 pA pF^{-1} in this experiment (2 mM Ca^{2+}, −100 mV step) was within 0.45 standard

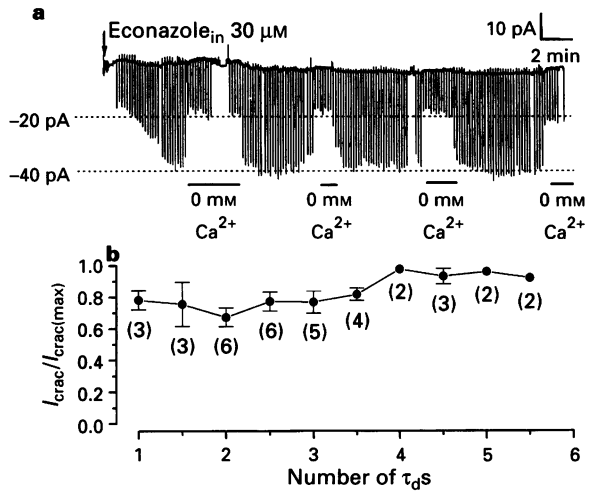

Figure 3 Lack of effect on I_{crac} of econazole dialysed intracellularly from the recording pipette during protracted whole cell recordings. (a) Continuous current trace during an extended (>29 min following achievement of the whole cell mode; arrow) recording with a pipette containing 30 μM econazole. Data were filtered at 50 Hz and digitized at 100 Hz. Negative deflections are current responses to −100 mV, 200 ms steps delivered at 0.1 Hz (holding potential: 0 mV). Ca^{2+} was transiently replaced with equimolar Mg^{2+} (0 mM Ca^{2+}) as indicated by bars. I_{crac} developed to an asymptotic amplitude ≈23 pA at −100 mV within 5 min of gaining whole cell access, and remained stable for the duration of the experiment. Measured series resistance was 15 MΩ, and whole cell capacitance was 19 pF, yielding a control peak I_{crac} density of 1.2 pA pF^{-1}. Econazole was estimated to equilibrate from the pipette to the cytosol at a monoexponential rate with a diffusion τ (τ_d) = 6.6 min (see Results). (b) Summary data from six extended recordings (duration: 18–34 min after break-in) by the protocol shown in (a), and 30 μM pipette econazole. In each experiment I_{crac} was normalized as a fraction of its maximal size, and time after gaining whole cell access was normalized as a number of estimated τ_ds. The mean ± s.e.mean (n in parentheses) normalized I_{crac} fractional values shown were obtained by binning amplitudes at 0.5 ± 0.15 τ_d increments. Normalized I_{crac} did not vary significantly over five econazole τ_ds (one-way ANOVA).

deviations of the mean current density obtained for control cells (1.51 ± 0.16 pA pF^{-1}; $n = 21$; see Figure 6), making it unlikely that a substantial portion of the current was rapidly blocked by econazole upon attainment of the whole cell mode (see below). I_{crac} amplitude remained stable for the remainder of the experiment. Leak current upon switching to Ca^{2+}-free buffer also did not vary by more than 10% throughout the recording in Figure 3a, or in the other experiments, arguing against a non-specific change in seal characteristics offsetting a coincidental decrease in the I_{crac} component of the total current.

Pusch & Neher (1988) previously described a procedure for estimating the diffusional exchange rate from a patch pipette to the cytosol, based on molecular mass of a compound, and the experimentally measured parameters of access resistance, and cell capacitance. We applied these calculations to provide a predicted diffusional τ value (τ_d) for each experiment where econazole was dialysed intracellularly. For the recording in Figure 3a a τ_d of 6.6 min was calculated for the econazole diffusional exchange rate, based on a measured cell capacitance of 19 pF, and series resistance of 15 MΩ. Therefore 4.4 τ_ds elapsed over the 29 min recording, leading to a predicted cytosolic econazole concentration of 28.6 μM at the end of the experiment. For the six extended experiments, 3.0–5.5 τ_ds (rounded to 0.5 τ_d) elapsed from break-in to the loss of the recording.

Possible changes in I_{crac} amplitude as a function of the number of elapsed τ_ds were determined for the prolonged recordings. I_{crac} amplitude at each time point was normalized to its maximal amplitude for each experiment. The normalized values were then binned across the cells at 0.5 ± 0.15 τ_d widths and averaged to yield a mean ± s.e.mean normalized I_{crac} amplitude at progressively increasing 0.5 τ_d intervals from the zero reference point (i.e., access to the whole cell mode; Figure 3b). The mean I_{crac} amplitudes did not vary significantly (one-way ANOVA) over 5.5 τ_ds. Thus there was no evidence for a progressive decrease in I_{crac} amplitude over a time period where econazole would be predicted by the Pusch & Neher (1988) diffusional calculation to achieve a cytosolic level close to the 30 μM pipette concentration.

To rule out a possible rapid initial block prior to the commencement of measurements, various discrete econazole concentrations (0.1, 1, 10 and 30 μM) were dialysed via the recording pipette in independent sets of experiments and the initial steady-state I_{crac} current density measured (Figure 4). The mean I_{crac} densities obtained from cells dialysed with the three different econazole concentrations did not differ significantly from one another or from the I_{crac} density in control cells (one-way ANOVA). These results argued that despite inclusion of econazole in the recording pipette, I_{crac} developed to predicted control current density, rather than being rapidly blocked immediately after the whole cell configuration had been achieved.

Effects of extracellularly applied econazole in econazole-dialysed cells

We evaluated quantitatively the extent of I_{crac} block produced by extracellularly applied econazole in cells that were also dialysed with pipette solutions containing 30 μM econazole. This approach was taken to confirm directly the sensitivity of I_{crac} to extracellularly applied econazole in the same cells where I_{crac} was apparently unaffected by internally applied econazole: if the lack of block actually resulted from a secondary, competing biochemical process invoked by a high concentration of econazole at an intracellular compartment, then the quantitative degree of block produced by the subsequent extracellular application would also be expected to be altered as a consequence.

Figure 5 shows the results of an experiment in which both intracellular econazole (30 μM) dialysis and extracellular econazole applications were used. I_{crac} developed to an asymptotic amplitude of 1.28 pA pF^{-1}. The τ_d predicted by the Pusch & Neher (1988) method in this cell was 2.9 min. Econazole (10 and 30 μM) was applied extracellularly beginning ≈6.5 min after break-in (2.3 τ_ds) resulting in a concentration-dependent I_{crac} block (19% at 10 μM and 58% at 30 μM). Current then slowly recovered to within 10% of the original control am-

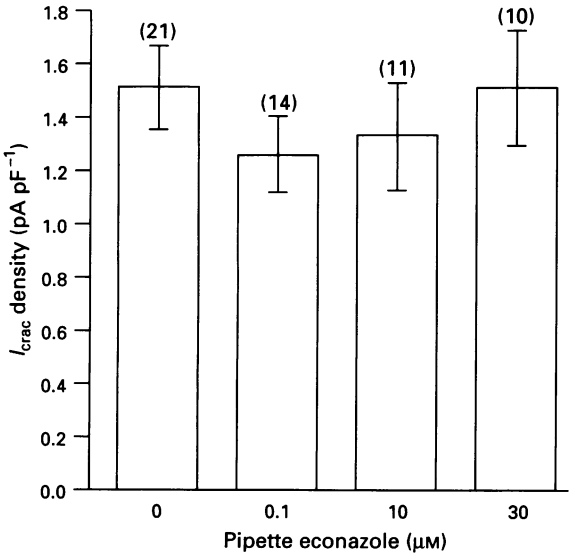

Figure 4 Comparison of I_{crac} densities between experiments with varying concentrations of pipette econazole (0.1–30 μM; 0 μM = Control). In each experiment peak I_{crac} was monitored with −100 mV steps; the protocol described for Figure 3a was used and current density determined when current developed to a steady-state level. Each column represents the mean ± s.e.mean (n in parentheses) steady-state I_{crac} density for the group of cells recorded with the pipette econazole concentration noted on the abscissa scale. No significant differences were indicated for mean I_{crac} density between the four groups (one-way ANOVA).

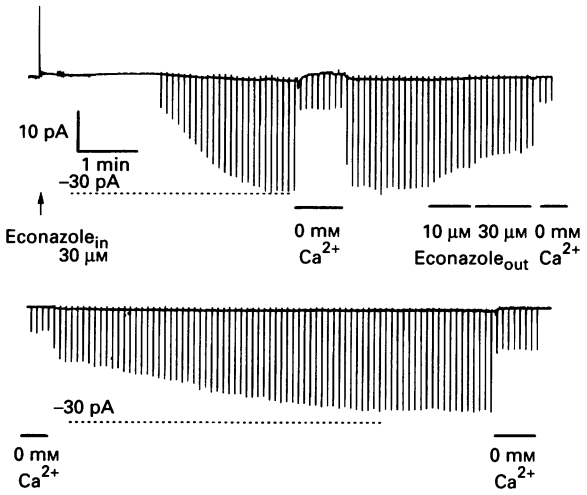

Figure 5 Concentration-dependent, reversible block of I_{crac} by extracellularly applied econazole in a cell recorded with a pipette containing 30 μM econazole. Upper and lower panels are contiguous and show an uninterrupted current record in an experiment where stability was maintained for ≈18 min after the whole cell mode was achieved (arrow: econazole$_{in}$ 30 μM). Data were filtered at 50 Hz and digitized at 200 Hz. Downward deflections are current responses to −100 mV, 200 ms steps delivered at 0.2 Hz (holding potential: 0 mV). Series resistance was 7 MΩ and whole cell capacitance was 18 pF, resulting in a steady-state I_{crac} density of 1.28 pA pF^{-1}, and an estimated τ_d of 2.9 min for diffusional exchange of econazole into the cytosol (see Methods). Ca^{2+} was transiently removed (0 Ca^{2+}), or increasing concentrations of econazole applied extracellularly as indicated by bars.

plitude within ≈9 min after removal of extracellular econazole even though intracellular dialysis of econazole continued. Transient removal of extracellular Ca^{2+} produced comparable leak current amplitudes early and late in the experiment, supporting the stability of the recording characteristics. This experiment was representative of three extended recordings which demonstrated that econazole applied extracellularly effectively and reversibly inhibited I_{crac} in the presence of intracellularly dialysed econazole.

I_{crac} block by extracellularly applied econazole concentrations (0.1 to 30 μM; extracellular econazole applied ≥2 τ_ds after break in) was quantitated by measuring current densities during the applications in all cells that were simultaneously dialysed with 30 μM econazole. The mean ± s.e.mean current densities from these cells were compared to those obtained from control cells (no internal econazole) during application of the same range of extracellular econazole concentrations (Figure 6). Current densities in both groups were reduced in a concentration-dependent manner by extracellular econazole. Greater variance was evident for these raw data values than for normalized % inhibition values obtained from these same control data (Figure 1c). The mean current densities obtained for the various econazole concentrations did not differ significantly between the two groups (two-way ANOVA). Thus intracellular application of a high econazole concentration did not affect either the threshold or the ultimate extent of I_{crac} block by external econazole.

I_{crac} *inhibition by econazole methiodide*

As an independent means to discriminate an extracellular vs. intracellular blocking site of econazole, we evaluated the inhibition on I_{crac} of econazole methiodide, a quaternary salt derivative of econazole. The substantial reduction in lipid solubility of econazole methiodide relative to econazole (≈2.5 orders of magnitude at pH 7.4 as indicated by log P values; see Methods) would be predicted to reduce the partitioning of the extracellularly applied compound into the membrane, and thereby greatly slow its rate of equilibration into the cytosol (Hille, 1977). Thus action at a putative intracellular site would be precluded over the typical timecourse of our experiments.

Econazole methiodide, when applied extracellularly at 1–30 μM, inhibited I_{crac} in a concentration-dependent manner (Figure 7a), albeit with a lower potency than econazole. The proportion of current blocked was 39 ± 3% (n = 13) at 30 μM, the highest concentration tested. This prevented an accurate IC_{50} determination within the 0.1 to 30 μM concentration range. The timecourse of block onset following extracellular application of 30 μM econazole was also examined in four cells. Block development was well fitted by monoexponential kinetics in the four cells (τ = 9.40 ± 1.6 s; Figure 7b). Thus the block onset kinetics for econazole methiodide appeared comparable to those observed for extracellularly applied econazole (Figure 2b). Given the seemingly reasonable assumption that the two compounds with highly similar structures, but considerably different partitioning coefficients acted at the same pharmacophore to inhibit I_{crac}, these results would support the hypothesis that this site is situated extracellularly.

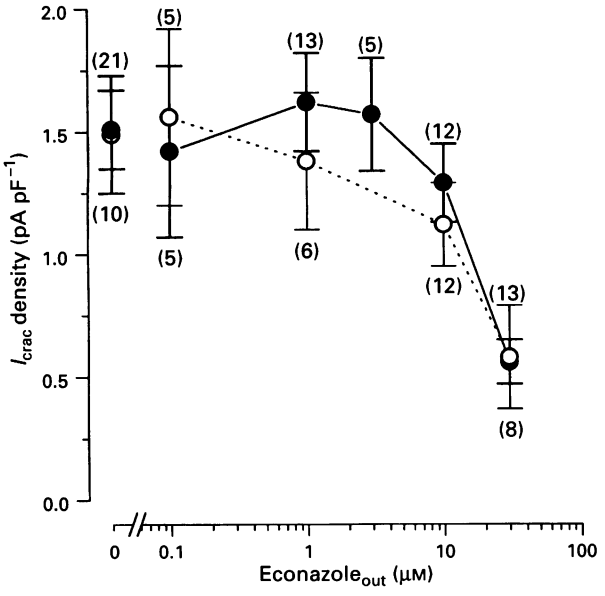

Figure 6 Quantitative comparison of effects on I_{crac} density of increasing extracellular econazole concentrations in cells recorded with control (●)- or 30 μM econazole (○)- containing pipette solutions. Semi-logarithmic concentration-response plot shows the mean ± s.e.mean (vertical lines) I_{crac} densities (n in parentheses above vertical lines for control, and below vertical lines for 30 μM econazole intracellular solutions) obtained for each group to the extracellularly applied econazole concentrations indicated on the abscissa scale. The mean current densities were significantly reduced as a function of increasing extracellular econazole concentration within both the control and 30 μM intracellular econazole treatment groups (P < 0.05 for each), but no significant effect existed between the two groups (2-way ANOVA).

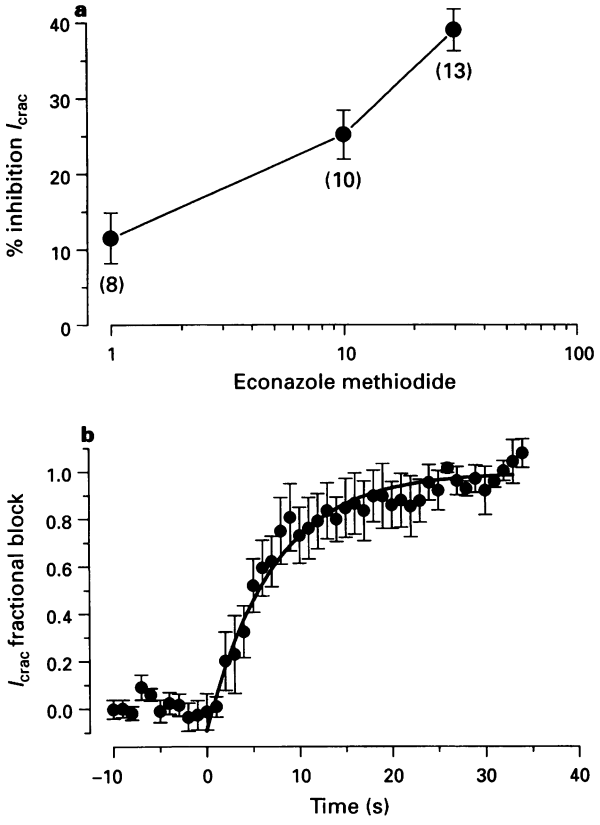

Figure 7 Characteristics of I_{crac} block by the quaternary econazole derivative, econazole methiodide. (a) Concentration-dependence of I_{crac} block by 1–30 μM econazole methiodide. Peak I_{crac} was measured in an experiment during −100 mV steps after steady-state block was achieved and this amplitude was normalized to the control current as a % inhibition value. Each point is the mean ± s.e.mean normalized current averaged from the number of experiments indicated in parentheses. (b) Kinetics for onset of I_{crac} block by 30 μM econazole methiodide. Experimental protocol, analytical procedure and graphical format are identical to those for Figure 2b with the exception that I_{crac} was monitored with −100 mV steps delivered at 1 Hz, rather than 0.5 Hz. Data points represent the mean and vertical lines the s.e.mean I_{crac} fractional block averaged from four experiments. The solid line is a monoexponential fit to the data (τ = 9.1 s).

Discussion

N_1-substituted imidazole antimycotics, such as econazole, are the most widely acknowledged class of organic blockers of capacitative Ca^{2+} entry, yet little information is available concerning the cellular or molecular mechanisms by which these inhibitors exert their effect. The data in the present study demonstrate directly for the first time that econazole blocks I_{crac} in the human T lymphocyte derived cell line, Jurkat. More importantly our data provide convergent evidence from two independent approaches that econazole does not block I_{crac} from an intracellular site or via a secondary intracellular biochemical mechanism, such as cytochrome P450 inhibition. Rather, the econazole-mediated block of I_{crac} appears to depend on its presence at an extracellular site, suggesting that this compound may interact directly with the channel protein itself.

Amongst the imidazole antimycotics, econazole has been shown to be one of the most potent inhibitors of capacitative Ca^{2+} entry, as measured by fluorometric techniques for free $Ca^{2+}{}_{in}$, or Mn^{2+} influx in a variety of cell types, including rat thymocytes (Alvarez *et al.*, 1991; 1992; Mason *et al.*, 1993; Koch *et al.*, 1994), human platelets (Alvarez *et al.*, 1991; Vostal & Fratantoni, 1993) and a human neutrophil-derived (i.e., HL-60) cell line (Koch *et al.*, 1994). The potency of econazole across these different cell types ranges consistently from submicromolar to below 10 μM values for block of one-half response. Moreover, econazole also shows submicromolar potency for blocking I_{crac} in rat peritoneal mast cells, as determined by direct patch clamp measurements (Franzius *et al.*, 1994). Data in the present study extend these prior findings by confirming that econazole blocks I_{crac} in a human-derived T cell line. That I_{crac} in Jurkat cells appears less sensitive to econazole (i.e., $IC_{50} = 13$ μM; Figure 1) than the capacitative Ca^{2+} entry pathways or I_{crac} in other cells evaluated in previous studies may reflect differences in experimental conditions, or alternatively, true pharmacological heterogeneity of I_{crac} channels. More extensive profiling with novel inhibitors as they become available will be necessary to clarify potential pharmacological differences in capacitative Ca^{2+} entry pathways. This information will be important for predicting the cell or tissue selectivity of I_{crac} blockers directed at desired therapeutic endpoints.

We were prompted to test the hypothesis of an intracellular action of econazole on I_{crac} based on a variety of information including: (1) the high lipophilicity of econazole, (2) the known effects of econazole for affecting intracellular biochemical pathways, particularly cytochrome P-450 enzymes with high potency (Murray & Zaluzny, 1988), and (3) the relatively slow onset rate (Figure 2) and protracted timecourse of reversal (Figure 5) we observed for econazole-mediated I_{crac} block.

Our strategy of applying econazole via the patch pipette follows the precedent of numerous other studies, some of the most notable being investigations of the site of action of phenylalkylamine- and dihydropyridine-based antagonists of L-type voltage-gated Ca^{2+} channels (for review, see Catterall & Striessning, 1992). Those studies were able to delineate through the approaches of intracellular dialysis and the use of quaternary derivatives of drugs that the phenylakylamine binding site resides on the intracellular side of the channel, and the dihydropyridine binding site on an extracellularly directed domain. Analogous to these previous studies with voltage-gated Ca^{2+} channel blockers, the conclusion against an intracellular site of econazole action obtained in the present study relies on the assumption that the compound in the pipette equilibrated effectively to the cytosol. We employed the quantitative methodology of Pusch & Neher (1988) to estimate the rate of diffusional exchange, based on experimentally measured parameters, and then monitored I_{crac} density in protracted experiments where nearly complete equilibration of econazole into the cytosol would be predicted (Figures 3 and 5). However, the Pusch & Neher (1988) estimation is subject to errors due to factors such as anomalies in the diffusional coefficient of a substance within the cytosol, as opposed to a pure aqueous solution, and high affinity partitioning or binding of the diffusing substance to an intracellular compartment.

Although we are unable to offer direct evidence that the intracellular econazole concentrations approached those predicted by the Pusch & Neher (1988) method, several indirect, but convergent lines of evidence support our ultimate conclusion against an intracellular blocking site. First, we failed to measure a quantitative effect of dialysing high concentrations of econazole on the reduction of I_{crac} density by a range of extracellular econazole concentrations (Figure 6). Some potentiation of the inhibition, particularly at low extracellular concentrations might have been expected, even if a lower than predicted econazole concentration reached a relevant intracellular site of action. Secondly, in several experiments with intracellularly dialysed econazole, the inhibition produced by extracellular econazole reversed nearly to control levels during a protracted period after econazole was removed from the extracellular solution (e.g., Figure 5). Finally, the observation that extracellular application of the considerably less lipophilic quaternary salt analogue, econazole methiodide, also blocked I_{crac} in a concentration-dependent manner and with similar onset kinetics to econazole (Figures 2 and 7) provides an independent argument against an intracellular site of action. This latter experimental strategy is precedented by the work of Hille (1977), who compared blocking on-rates to delineate extracellular and intracellular sites of block on axonal Na channels by local anaesthetics and their quaternary salt derivatives.

Our data provide a strong argument against the hypothesis that cytochrome P-450 inhibition is involved in the mechanism of econazole-mediated block of capacitative Ca^{2+} entry (Alonso *et al.*, 1991; Alvarez *et al.*, 1991; 1992; Montero *et al.*, 1991; Sargeant *et al.*, 1992). Moreover, the present results are incompatible with the associated hypothesis implicating cytochrome P-450 in the signalling pathway between Ca^{2+} depletion of microsomal stores and activation of capacitative Ca^{2+} entry. Two earlier studies provided evidence incompatible with the hypothesis linking cytochrome P-450 to regulation of capacitative Ca^{2+} influx. Vostal & Fratantoni (1993) demonstrated that irreversible inhibition of cytochrome P-450 by CO had no measurable effect on capacitative Ca^{2+} entry in platelets. Likewise, Koch *et al.* (1994) prepared chemical derivatives of econazole that dissociated the inhibitory effects on cytochrome P-450 with the block of capacitative Ca^{2+} entry in HL-60 cells: chemical derivatives practically devoid of inhibitory activity on cytochrome P-450 retained the ability to block Ca^{2+} influx. The present study provides strong corroboration of these earlier findings by way of direct measurements of I_{crac}, and thus strengthens considerably the argument against cytochrome P-450 involvement in the activation or modulation of capacitative Ca^{2+} entry.

In conclusion, our findings make an important contribution to the relatively diminutive information base that is available concerning the pharmacology of capacitative Ca^{2+} entry channels. We demonstrated through convergent results (i.e., intracellular econazole dialysis, econazole methiodide effects) that the prototypical inhibitor, econazole, blocks I_{crac} from an extracellular rather than intracellular site in a human T lymphocyte derived cell line. Thus despite the relatively low potency of econazole for I_{crac} block, and its known lack of specificity in inhibiting a variety of other ion channel types (Franzius *et al.*, 1994), our results support the hypothesis that this compound inhibits I_{crac} by interacting directly with an extracellularly directed domain of the channel protein, rather than by affecting intracellular biochemical events. In particular, our findings argue that econazole-mediated inhibition of capacitative Ca^{2+} entry is distinct from its known inhibitory effects on cytochrome P-450.

We wish to thank P. Bradley for performing the log P measurements for econazole and econazole methiodide. We thank Drs J.H. Li and M. Hoth for their critical comments on an earlier draft of this manuscript.

References

ALONSO, M.T., ALVAREZ, J., MONTERO, M., SANCHEZ, A. & GARCÍA-SANCHO, J. (1991). Agonist-induced Ca^{2+} influx into human platelets is secondary to the emptying of intracellular calcium stores. *Biochem. J.*, **280,** 783–789.

ALVAREZ, J., MONTERO, M. & GARCÍA-SANCHO, J. (1991). Cytochrome P-450 may link intracellular Ca^{2+} stores with plasma membrane Ca^{2+} influx. *Biochem. J.*, **274,** 193–197.

ALVAREZ, J., MONTERO, M. & GARCÍA-SANCHO, J. (1992). Cytochrome P450 may regulate plasma membrane Ca^{2+} permeability to the filling state of the intracellular Ca^{2+} stores. *FASEB J.*, **6,** 786–792.

BALLARD, S.A., LODOLA, A. & TARBIT, M.H. (1988). A comparative study of 1-substituted imidazole and 1,2,4-triazole antifungal compounds as inhibitors of testosterone hydroxylations catalysed by mouse hepatic microsomal cytochromes P-450. *Biochem. Pharmacol.*, **37,** 4643–4651.

BARRY, P.H. & LYNCH, J.W. (1991). Liquid junction potentials and small cell effects in patch clamp analysis. *J. Membr. Biol.*, **121,** 101–117.

CATTERALL, W.A. & STRIESSNING, J. (1992). Receptor sites for Ca^{2+} channel antagonists. *Trends Pharmacol. Sci.*, **13,** 256–262.

CHRISTIAN, E.P., SPENCE, K.T., TOGO, J.A., DARGIS, P.G. & PATEL, J. (1996). Calcium-dependent enhancement of depletion-activated calcium current in Jurkat T lymphocytes. *J. Membr. Biol.*, **150,** 63–71.

CHRISTIAN, E.P., TOGO, J.A., SPENCE, K.T. & DARGIS, P.G. (1995). Econazole blocks depletion-activated Ca^{2+} current in Jurkat cells from an extracellular site. *Biophys. J.*, **68,** A207.

CHUNG, S.C., MCDONALD, T.V. & GARDNER, P. (1994). Inhibition by SK&F 96365 of Ca^{2+} current, IL-2 production and activation in T lymphocytes. *Br. J. Pharmacol.*, **113,** 861–868.

FRANZIUS, D., HOTH, M. & PENNER, R. (1994). Non-specific effects of calcium entry antagonists in mast cells. *Pflügers Arch Eur. J. Physiol.*, **428,** 433–438.

HAMILL, O.P., MARTY, A., NEHER, E., SAKMANN, B. & SIGWORTH, F.J. (1981). Improved patch-clamp techniques for high-resolution recording from cells and cell-free membrane patches. *Pflügers Arch.*, **391,** 85–100.

HILLE, B. (1977). The pH-dependent rate of action of local anesthetics on the node of Ranvier. *J. Gen. Physiol.*, **69,** 475–496.

HOTH, M. & PENNER, R. (1992). Depletion of intracellular calcium stores activates a calcium current in mast cells. *Nature*, **355,** 353–356.

HOTH, M. & PENNER, R. (1993). Calcium release-activated calcium current in mast cells. *J. Physiol.*, **465,** 359–386.

KOCH, B.D., FAUROT, G.F., KOPANITSA, M.V. & SWINNEY, D.C. (1994). Pharmacology of Ca^{2+}-influx pathway activated by emptying the intracellular Ca^{2+} stores in HL-60 cells: evidence that a cytochrome P-450 is not involved. *Biochem. J.* **302,** 187–190.

LEWIS, R.S. & CAHALAN, M.D. (1989). Mitogen-induced oscillations of cytosolic Ca^{2+} and transmembrane Ca^{2+} current in human leukemic T cells. *Cell Regulation*, **1,** 99–112.

MASON, M.J., MAYER, B. & HYMEL, L.J. (1993). Inhibition of Ca^{2+} transport pathways in thymic lymphocytes by econazole, miconazole, and SKF 96365. *Am. J. Physiol.*, **264** (*Cell Physiol.*, **33**), C654–C662.

MCDONALD, T.V., PREMACK, B.A. & GARDNER, P. (1993). Flash photolysis of caged inositol 1,4,5-trisphosphate activates plasma membrane calcium current in human T cells. *J. Biol. Chem.*, **268,** 3889–3896.

MERRITT, J.E., ARMSTRONG, W.P., BENHAM, C.D., HALLAM, T.J., JACOB, R., JAXA-CHAMIEC, A., LEIGH, B.K., MCCARTHY, S.A., MOORES, K.E. & RINK, T.J. (1990). SK&F96365, a novel inhibitor of receptor-mediated Ca^{2+} entry. *Biochem. J.*, **271,** 515–522.

MONTERO, M., ALVAREZ, J. & GARCÍA-SANCHO, J. (1991). Agonist-induced Ca^{2+} influx in human neutrophils is secondary to the emptying of intracellular calcium stores. *Biochem. J.* **277,** 73–79.

MURRAY, M. & ZALUZNY, L. (1988). Comparative effects of antithrombitic and antimycotic N-substituted imadazoles on rat hepatic microsomal steroid and xenobiotic hydroxylases *in vitro*. *Biochem. Pharmacol.*, **37,** 415–420.

PREMACK, B.A., MCDONALD, T.V. & GARDNER, P. (1994). Activation of Ca^{2+} current in Jurkat T cells following the depletion of Ca^{2+} stores by microsomal Ca^{2+}-ATPase inhibitors. *J. Immunol.*, **152,** 5226–5240.

PUSCH, M. & NEHER, E. (1988). Rates of diffusional exchange between small cells and a measuring patch pipette. *Pflügers Arch Eur. J. Physiol.*, **411,** 204–211.

PUTNEY, J.W. Jr. (1990). Capacitative Ca^{2+} entry revisited. *Cell Calcium*, **11,** 611–624.

RODRIGUES, A.D., GIBSON, G.G., IOANNIDES, C. & PARKE, D.V. (1987). Interactions of imidazole antifungal agents with purified cytochrome P-450 proteins. *Biochem. Pharmacol.*, **36,** 4277–4281.

SARGEANT, P., CLARKSON, W.D., SAGE, S.O. & HEEMSKERK, J.W.M. (1992). Calcium influx evoked by Ca^{2+} store depletion in human platelets is more susceptible to cytochrome P-450 inhibitors than receptor-mediated calcium entry. *Cell Calcium*, **13,** 553–564.

VOSTAL, J.G. & FRATANTONI, J.C. (1993). Econazole inhibits thapsigargan-induced platelet calcium influx by mechanisms other than cytochrome P-450 inhibitions. *Biochem. J.*, **295,** 525–529.

ZWEIFACH, A. & LEWIS, R.S. (1993). Mitogen-regulated Ca^{2+} current of T lymphocytes is activated by depletion of intracellular Ca^{2+} stores. *Proc. Natl. Acad. Sci. U.S.A.*, **90,** 6295–6299.

ZWEIFACH, A. & LEWIS, R.S. (1995). Rapid inactivation of depletion-activated calcium current (I_{crac}) due to local calcium feedback. *J. Gen. Physiol.*, **105,** 209–226.

(Received April 29, 1996
Revised July 3, 1996
Accepted July 12, 1996)